

Figure 1. The modified Morse function $V(r - r_0) = D_0[\exp\{-2B(r - r_0)\} - 2n^q \exp\{-B(r - r_0)\}]$ (eq 5) with $D_0 = 100 \text{ kcal mol}^{-1}$, $B = 2 \text{ \AA}^{-1}$, $q = 1$, $n = 1$ (outer curve), 0.9, 0.8. Note the sharp decrease in dissociation energy as the equilibrium distance increases (compare eq 10).

a unifying thread connecting changes in bond energy, bond distance, and stretching force constants.

The connection between bond distance and energy (eq 10) is particularly interesting and important, because it provides a ra-

tionale for the astonishingly sharp sensitivity of activation energy of bond-breaking processes to quite small changes in ground-state geometry^{11,12} (Figure 1). With $\partial\Delta G^\ddagger/\partial r$ values of the order of 200–300 $\text{kcal mol}^{-1} \text{ \AA}^{-1}$, bond length differences of a few hundredths of an Å between corresponding bonds in related structures should have a profound influence on the rates of corresponding bond-breaking reactions.¹⁷ This connection underlines the need for accurate bond length measurements in structural studies bearing on questions of chemical reactivity.¹⁹ Since careful X-ray diffraction studies, especially at low temperatures, are perfectly capable of determining interatomic distances with a precision of the order of 0.001–0.002 Å, interesting results can be expected in this direction.

Another problem of interest is the dependence of ground-state structure on bond environment factors such as hydrogen bonding, donor–acceptor interactions, stereoelectronic effects, etc. and the consequences for reactions involving bond breaking. In particular, we envisage that binding of a substrate to the active site of an enzyme may be accompanied by small structural changes that could have dramatic effects on reaction rate.

(17) Of course, the identification of $\partial\Delta G^\ddagger/\partial r$ with $\partial D(r_e)/\partial r_e$ is valid only insofar as $\partial\Delta S^\ddagger/\partial r$ is small. In the few cases where $\partial\Delta H^\ddagger/\partial r$ and $\partial\Delta G^\ddagger/\partial r$ values are available they are indeed not very different.^{12,18}

(18) Müller, E.; Bürgi, H. B. *Helv. Chim. Acta*, in press.

(19) For example, the retardation of the rate of aquation of $[\text{Cr}(\text{NH}_2\text{Me})_3\text{Cl}]^{2+}$ as compared with $[\text{Cr}(\text{NH}_3)_5\text{Cl}]^{2+}$ can be explained²⁰ in terms of the shorter Cr–Cl bond length found for the former, 2.299 (1) vs. 2.327 (1) Å for the latter. This interpretation runs counter to previous arguments that ascribed the difference in rate constant to a difference in reaction mechanism.

(20) Lay, P. A. *J. Chem. Soc., Chem. Commun.* 1986, 1422.

On the Nature of the Low-Lying Electronic Levels of a Tetranuclear Copper(II) Complex

Alessandro Bencini,^{1a} Dante Gatteschi,^{*1b} Claudia Zanchini,^{1b} Jaap G. Haasnoot,^{1c} Rob Prins,^{1c} and Jan Reedijk^{*1c}

Contribution from the Department of Chemistry, University of Florence, I.S.S.E.C.C., C.N.R., Florence, Italy, and the Department of Chemistry, State University Leiden, Gorlaeus Laboratories, Leiden, The Netherlands. Received August 26, 1986

Abstract: The magnetic susceptibility and the EPR spectra of tetrakis[aqua(3-(pyridin-2-yl)-5-(pyrazin-2-yl)-1,2,4-triazolato)copper(II)] tetranitrate dodecahydrate (I) were recorded in the temperature range 4.2–300 K. The magnetic data show that the four copper(II) ions are antiferromagnetically coupled. The temperature dependence of the magnetic susceptibility was fit with $J' = 12.2 \text{ cm}^{-1}$ (spin Hamiltonian in the form $\mathcal{H} = J'S_1 \cdot S_2$). The room-temperature EPR spectra are satisfactorily analyzed as due to an $S = 2$ species, with $g_{\parallel} = 2.03$, $g_{\perp} = 2.16$, and $|D| = 0.0379 \text{ cm}^{-1}$, while the spectra obtained at 4.2 K are typical of a triplet with $g_{\parallel} = 2.03$, $g_{\perp} = 2.16$, and $|D| = 0.0906 \text{ cm}^{-1}$. The spin-Hamiltonian parameters are interpreted within a model which relates them to the corresponding parameters of the individual ions and to the exchange and dipolar contributions.

The exchange interactions between paramagnetic centers have been actively investigated in the last few years.² As a conclusion of this research we can say that much is now understood of the details of the interaction in pairs, where the role of both the ground^{3–11} and the excited^{12–15} magnetic orbitals has been fully

clarified, providing a set of rules which extends the original Goodenough–Kanamori rules^{16,17} and allowing the rationalization

(1) (a) I.S.S.E.C.C., C.N.R. (b) University of Florence. (c) State University Leiden.

(2) *Magneto-Structural Correlations in Exchange Coupled Systems*; Willett, R. D., Gatteschi, D., Kahn, O., Eds.; D. Reidel: Dordrecht, Holland, 1985.

(3) Kahn, O. *Angew. Chem., Int. Ed. Engl.* 1985, 24, 834.

(4) Hatfield, W. E. In ref 2, p 555.

(5) Kahn, O. In ref 2, p 37.

(6) Daudey, J. P.; de Loth, P.; Malrieu, J. P. In ref 2, p 87.

(7) Willett, R. D. In ref 2, p 389.

(8) Hodgson, D. J. In ref 2, p 497.

(9) Hendrickson, D. N. In ref 2, p 523.

(10) Solomon, E. I.; Wilcox, D. E. In ref 2, p 463.

(11) Gatteschi, D.; Bencini, A. In ref 2, p 241.

(12) Banci, L.; Bencini, A.; Gatteschi, D. *J. Am. Chem. Soc.* 1983, 105, 761.

(13) Bencini, A.; Gatteschi, D.; Zanchini, C. *Inorg. Chem.* 1985, 24, 704.

(14) Charlot, M. F.; Journaux, Y.; Kahn, O.; Bencini, A.; Gatteschi, D.; Zanchini, C. *Inorg. Chem.* 1986, 25, 1060.

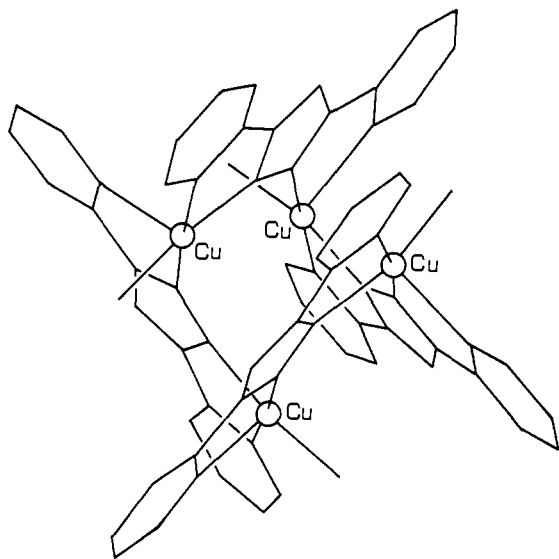


Figure 1. Schematic view of the Cu_4 cluster in tetrakis[aqua(3-(pyridin-2-yl)-5-(pyrazin-2-yl)-1,2,4-triazolato)copper(II)] tetranitrate dodecahydrate (I).

of the magnetic properties for virtually any magnetic center in any geometry.

At the other limit, a good understanding has been obtained also for the magnetic interactions in infinite lattices,¹⁸⁻²² either one-, two-, or three-dimensional, for which both the thermodynamic and the dynamic properties have been successfully rationalized and the relations between structural and magnetic dimensionality have been discussed at length.

When we look at the vast field of clusters which fall in between these two limits, we find that, although in broad lines the magnetic properties are understood, much of the detail has not yet been analyzed. For instance, we can generally explain the magnetic susceptibility of these systems, but we do not have any detailed knowledge of the different total spin states which are thermally populated. There is increasing interest in this area for the relevance that these systems have to many different problems. Indeed clusters of three and four paramagnetic ions are present in iron-sulfur proteins,²³⁻²⁵ oligonuclear iron complexes are relevant to both biological iron storage and corrosion problems,²⁶ systems involving paramagnetic metal ions and organic radicals are investigated²⁷⁻³⁰ also to shed light on the mechanism of photosynthesis, high-spin clusters are studied as possible building blocks of novel magnetic materials,³¹ and organic polyradicals are synthesized and characterized.³²

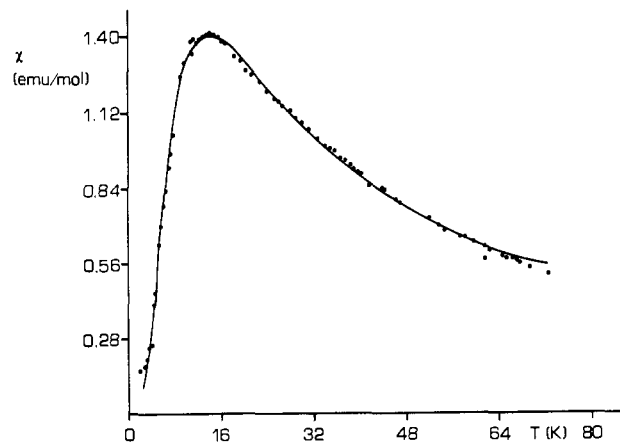


Figure 2. Temperature dependence of the magnetic susceptibility of tetrakis[aqua(3-(pyridin-2-yl)-5-(pyrazin-2-yl)-1,2,4-triazolato)copper(II)] tetranitrate dodecahydrate (I), in the form χ vs. T .

In particular, tetranuclear metal compounds have up to now resisted all attempts to obtain a detailed knowledge of the low-lying energy levels,³³ even though they include systems of great interest, such as the 4Fe-4S proteins. Also in the relatively simple case of four copper(II) ions, where four $S = 1/2$ states are coupled to give a quintet, three triplet, and two singlet electronic levels, many difficulties have been encountered, and still much controversy is present in the literature concerning the relative order of the various multiplets.³⁴⁻⁴⁶

In search for a tetranuclear system that allows EPR study, one should first of all consider ligands that are so large that interaction between cluster in the crystal lattice is very small, to avoid extra complications such as the exchange narrowing. Further, the magnetic exchange in the cluster should be sufficiently large to result in clear splittings of the ground-state levels, but not too large to avoid diamagnetism. It appeared that the tetranuclear compound tetrakis[aqua(3-(pyridin-2-yl)-5-(pyrazin-2-yl)-1,2,4-triazolato)copper(II)] tetranitrate dodecahydrate (I), of which the crystal structure was recently reported,⁴⁷ ideally fulfils these requirements, particularly because the symmetry of the cluster is S_4 . A schematic view of the Cu_4 cluster is given in Figure 1. The structure of the tetranuclear unit consists of an arrangement of four copper(II) ions on the vertices of a slightly distorted tetrahedron. The coordination geometry around the copper ions is distorted square pyramidal.

We decided to study the magnetic properties and the EPR

- (15) Moriya, T. *Phys. Rev.* **1960**, *120*, 91.
 (16) Goodenough, J. B. In *Magnetism and the Chemical Bond*; Interscience: New York, 1963.
 (17) (a) Kanamori, J. In *Magnetism*; Rado, G. T., Suhl, H., Eds.; Academic Press: New York, 1963; Vol. 1, p 161. (b) Kanamori, J. *J. Phys. Chem. Solids* **1959**, *10*, 87.
 (18) De Jongh, L. J. In ref 2, p 1.
 (19) Willett, R. D. In ref 2, p 269.
 (20) Bonner, J. C. In ref 2, p 159.
 (21) Hatfield, W. E.; Estes, V. E.; Mash, W. E.; Pickens, M. W.; Ter Haar, L. W.; Weller, R. R. In *Extended Linear Chain Systems*; Miller, J. S., Ed.; Plenum Press: New York, 1982; Vol. 3, p 43.
 (22) Willett, R. D.; Gaura, R. M.; Landee, C. P. In ref 21, p 143.
 (23) Berg, J. M.; Holm, R. H. In *Iron Sulfur Proteins*; Spiro, T. G., Ed.; Wiley, New York, 1982, p 1.
 (24) Orme-Johnson, W. H.; Orme-Johnson, N. R. In ref 23, p 67.
 (25) Münck, E. In ref 23, p 147.
 (26) Lippard, S. J. *Chem. Brit.* **1986**, 222.
 (27) Eaton, S. S.; Eaton, G. R. *Coord. Chem. Rev.* **1978**, *26*, 207.
 (28) Benelli, C.; Gatteschi, D.; Zanchini, C.; Doedens, R. J.; Dickman, M. H.; Porter, L. C. *Inorg. Chem.*, in press.
 (29) Lynch, M. W.; Hendrickson, D. N.; Fitzgerald, B. J.; Pierpont, C. G. *J. Am. Chem. Soc.* **1984**, *106*, 2041.
 (30) Mathur, P.; Dismukes, G. C. *J. Am. Chem. Soc.* **1983**, *105*, 7093.
 (31) Pey, T.; Journaux, Y.; Kahn, O.; Dei, A.; Gatteschi, D. *J. Chem. Soc., Chem. Commun.* **1986**, 1300.

- (32) Teki, Y.; Takui, T.; Itoh, K.; Iwamura, H.; Kobayashi, K. *J. Am. Chem. Soc.* **1986**, *108*, 2147.
 (33) Haase, W.; Walz, L.; Nepveu, F. In *The Coordination Chemistry of Metalloenzymes*; Bertini, I., Drago, R. S., Luchinat, C., Eds.; D. Reidel: Dordrecht, Holland, 1983; p 229.
 (34) Buluggiu, E. *J. Chem. Phys.* **1986**, *84*, 1243.
 (35) Buluggiu, E. *J. Chem. Phys.* **1985**, *83*, 5345.
 (36) Black, T. D.; Rubins, R. S.; De, D. K.; Dickinson, R. C.; Baker, W. A., Jr. *J. Chem. Phys.* **1984**, *80*, 4620.
 (37) Jones, D. H.; Sams, J. R.; Thompson, R. C. *Inorg. Chem.* **1983**, *22*, 1399.
 (38) ten Hoedt, R. W. M.; Hulsbergen, F. B.; Verschoor, G. C.; Reedijk, J. *Inorg. Chem.* **1982**, *21*, 2369.
 (39) Wong, H.; tom Dieck, H.; O'Connor, C. J.; Sinn, E. *J. Chem. Soc., Dalton Trans.* **1980**, 786.
 (40) Lines, M. E.; Ginsberg, A. P.; Martin, R. L.; Sherwood, R. C. *J. Chem. Phys.* **1972**, *57*, 1.
 (41) Stankowski, J.; Mackowiak, M. *Phys. Status Solidi* **1972**, *51*, 449.
 (42) Waplak, S.; Schmidt, V. H.; Drumheller, J. E. *Phys. Rev. B* **1985**, *32*, 48.
 (43) Polinger, V. Z.; Chibotaru, L. F.; Bersuker, I. B. *Sov. Phys. Solid State* **1984**, *26*, 345.
 (44) Polinger, V. Z.; Chibotaru, L. F.; Bersuker, I. B. *Mol. Phys.* **1984**, *52*, 1271.
 (45) Polinger, V. Z.; Chibotaru, L. F.; Bersuker, I. B. *Phys. Status Solidi B* **1985**, *129*, 615.
 (46) *Copper Coordination Chemistry: Biochemical and Inorganic Perspectives*; Karlin, K. D., Zubieta, J., Eds.; Adenine Press: Guilderland, NY, 1983.
 (47) Prins, R.; De Graaff, R. A. G.; Haasnoot, J. G.; Vader, C.; Reedijk, J. *J. Chem. Soc., Chem. Commun.*, in press.

spectra of I in the range 4.2–300 K in order to fully characterize the low-lying energy levels and the anisotropic exchange in the various spin multiplets.

Experimental Section

The magnetic susceptibility data of the cluster were collected on a vibrating sample magnetometer (PAR Model 150A) in the temperature range 2–80 K using tetrakis(thiocyanato)mercury cobaltate as a susceptibility standard. The experimental susceptibility data were corrected for the underlying diamagnetism (200×10^{-6} emu per mol of Cu) using Pascal constants.

EPR spectra of tetrakis[aqua(3-(pyridin-2-yl)-5-(pyrazin-2-yl)-1,2,4-triazolato)copper(II)] tetranitrate dodecahydrate (I) were recorded with a Bruker ER200 and a Varian E9 spectrometer at X and Q band, respectively. Low-temperature spectra were obtained with the use of an Oxford Instruments ESR9 continuous-flow cryostat. EPR-suitable single crystals of the title compound were oriented with a Philips PW 1100 diffractometer and were found to have a well-developed (110) face.

Results

The magnetic susceptibility of I increases steadily with decreasing temperature until it reaches a maximum at 13.5 K, as shown in Figure 2. Below this temperature the susceptibility decreases again, in agreement with a diamagnetic ground state, leading to an overall antiferromagnetic exchange interaction. The increase of the susceptibility at the lowest temperatures that could be reached is indicative of a small amount of impurity of a paramagnetic copper(II) species.

Using the isotropic part of the exchange Hamiltonian, six thermally populated levels can be obtained from which a theoretical expression for the susceptibility per mole of Cu can be obtained. This expression, where the lowest lying state of the energy diagram (the $S = 0$ state) is normalized at zero on the energy scale, and where $x = -J'/2kT$ and $y = -J/2kT$, is the following:

$$\chi_{\text{Cu}} = \frac{Ng^2\beta^2}{2kT} \times \frac{5 \exp(6x) + \exp(2x) + 2 \exp(4x - 2y)}{1 + 5 \exp(6x) + 3 \exp(2x) + 6 \exp(4x - 2y) + \exp(4x - 4y)}$$

where J refers to the exchange interaction Cu1 – Cu3 and Cu2 – Cu4, and J' to all the other copper–copper interactions (see below). The calculated susceptibility χ_{calcd} consist of χ_{Cu} , χ_{para} , and χ_{TIP} , where χ_{para} comes from the presence of paramagnetic impurities and χ_{TIP} comes from the temperature-independent paramagnetism, for which a value of 60×10^{-6} emu mol $^{-1}$ is taken. The calculated susceptibility therefore becomes:

$$\chi_{\text{calcd}} = (1 - \rho)\chi_{\text{Cu}} + \chi_{\text{para}} + \chi_{\text{TIP}}$$

The experimental data were fitted to this equation by means of a Simplex routine,⁴⁸ minimizing the sum of $(\chi_{\text{expt}} - \chi_{\text{calcd}})^2$, obtaining $g = 2.17$, $J' = 12.2$ cm $^{-1}$, $J = -0.6$ cm $^{-1}$, and $\rho = 0.002$.

The polycrystalline powder EPR spectra of I at room temperature are shown in Figure 3 at X- and Q-band frequency, respectively. Their interpretation is not straightforward, but they become immediately clear if they are compared with the results of the single-crystal spectra shown in Figure 4. Because of the tetragonal symmetry of the crystals and of the S_4 site symmetry of the Cu $_4$ clusters, only two orientations in the external static magnetic field are required,⁴⁹ namely, parallel and perpendicular to the c crystal axis. In both cases a quartet is observed, with no other transition resolved. These spectra are satisfactorily analyzed as due to an $S = 2$ species, with $g_{\parallel} = 2.03$, $g_{\perp} = 2.16$, and $|D| = 0.0379$ cm $^{-1}$, neglecting fourth-order corrections. The intensity distribution of the four lines follows the well-known behavior.⁵⁰ The angular dependence of the resonance fields is also in agreement with this assignment.

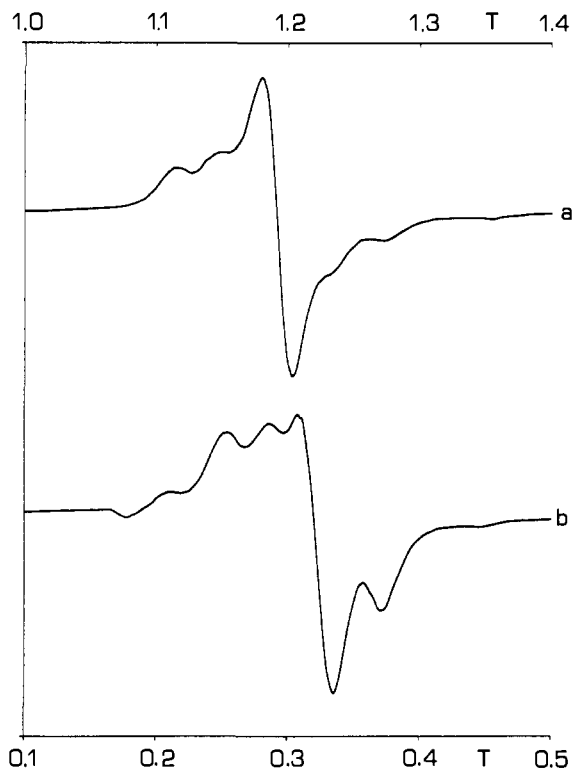


Figure 3. Polycrystalline powder EPR spectra of I at room temperature: (a) Q-band frequency (35 GHz), (b) X-band frequency (9.60 GHz).

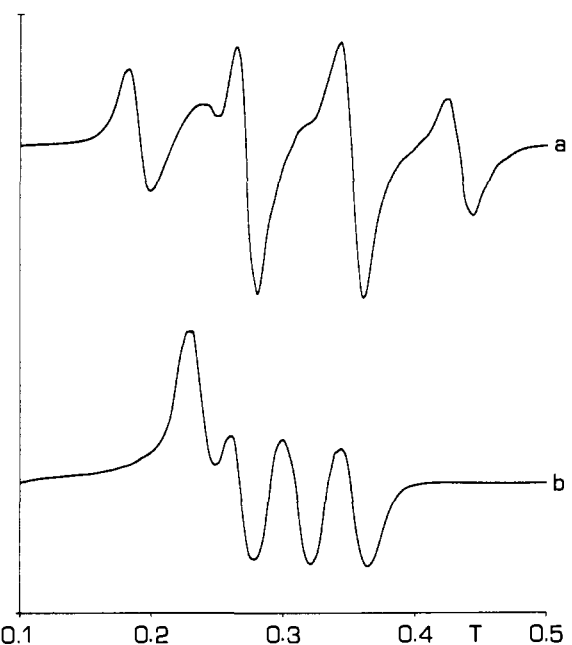


Figure 4. Single-crystal spectra of I at room temperature at X-band frequency (9.60 GHz), with the static magnetic field (a) parallel to the c axis and (b) orthogonal to the c axis.

Although the spectra sharpen up a little on cooling, no substantial change is observed on cooling down to liquid nitrogen temperature. On further cooling, the high-temperature spectrum decreases in intensity and eventually vanishes. The polycrystalline powder EPR spectrum at X-band frequency at 4.2 K is shown in Figure 5. It is completely different from the high-temperature spectra, with features at ca. 150, 220, 260, 340, and 420 mT which are typical of a triplet. The features at ca. 100 and 300 mT are not easily understood.

The single-crystal spectra at 4.2 K, shown in Figure 6, confirm the assignment of the triplet features, with $g_{\parallel} = 2.03$, $g_{\perp} = 2.16$, and $|D| = 0.0906$ cm $^{-1}$. The spectra orthogonal to the c axis were

(48) Olsson, D. M. *J. Qual. Technol.* 1974, 6, 53.

(49) Bencini, A.; Gatteschi, D. *Transition Met. Chem. (N.Y.)* 1982, 8, 1.

(50) Weltner, W., Jr. *Magnetic Atoms and Molecules*; Scientific and Academic Edition: New York, 1983.

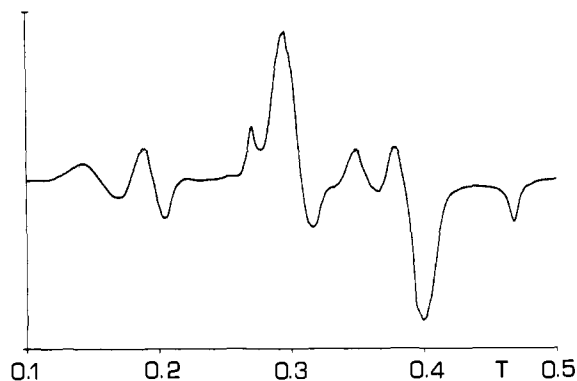


Figure 5. Polycrystalline powder EPR spectra of I at 4.2 K at X-band frequency (9.05 GHz).

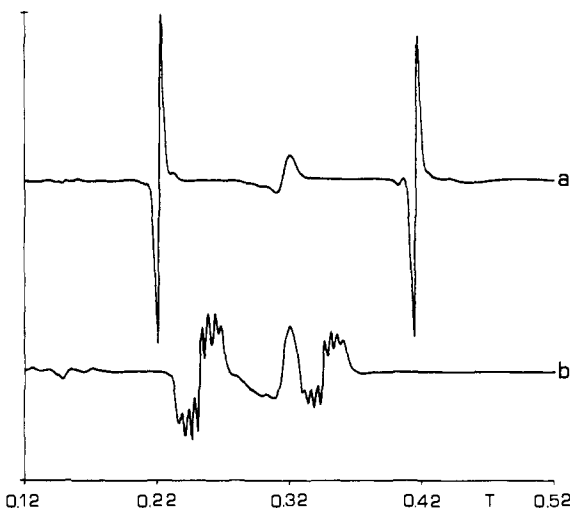


Figure 6. Single-crystal spectra of I at 4.2 K at X-band frequency (9.05 GHz), with the static magnetic field (a) parallel to the c axis and (b) orthogonal to the c axis.

recorded parallel to Y , the perpendicular to the $(1\bar{1}0)$ face. In this orientation both the $\Delta M = \pm 1$ and $\Delta M = \pm 2$ transitions show a hyperfine splitting into seven lines, as would be expected for two equivalent copper ions. A_{\perp} is found to be 0.045 cm^{-1} . Another important characteristic of the low-temperature spectra is that satellites are observed around the sharp $\Delta M = \pm 1$ transitions parallel to c . The two satellites are separated by approximately 22 mT and are markedly anisotropic in line width, as shown in Figure 6.

The feature at ca. 300 mT is independent of field orientation, with a shape reminiscent of a polycrystalline powder spectrum. The feature at ca. 100 mT is much less intense, so that it is difficult to follow, but it seems to be essentially independent of field orientation.

Discussion

The spin Hamiltonian appropriate for the exchange interaction of the four-spin $S = 1/2$ with S_4 symmetry can be written as:

$$\mathcal{H} = J(\mathbf{S}_1 \cdot \mathbf{S}_3 + \mathbf{S}_2 \cdot \mathbf{S}_4) + J'(\mathbf{S}_1 \cdot \mathbf{S}_2 + \mathbf{S}_1 \cdot \mathbf{S}_4 + \mathbf{S}_2 \cdot \mathbf{S}_3 + \mathbf{S}_3 \cdot \mathbf{S}_4) + \mathbf{S}_1 \cdot \mathbf{D}_{12} \cdot \mathbf{S}_2 + \mathbf{S}_1 \cdot \mathbf{D}_{13} \cdot \mathbf{S}_3 + \mathbf{S}_1 \cdot \mathbf{D}_{14} \cdot \mathbf{S}_4 + \mathbf{S}_2 \cdot \mathbf{D}_{23} \cdot \mathbf{S}_3 + \mathbf{S}_2 \cdot \mathbf{D}_{24} \cdot \mathbf{S}_4 + \mathbf{S}_3 \cdot \mathbf{D}_{34} \cdot \mathbf{S}_4 \quad (1)$$

where the numbering scheme is shown below: In the limit of

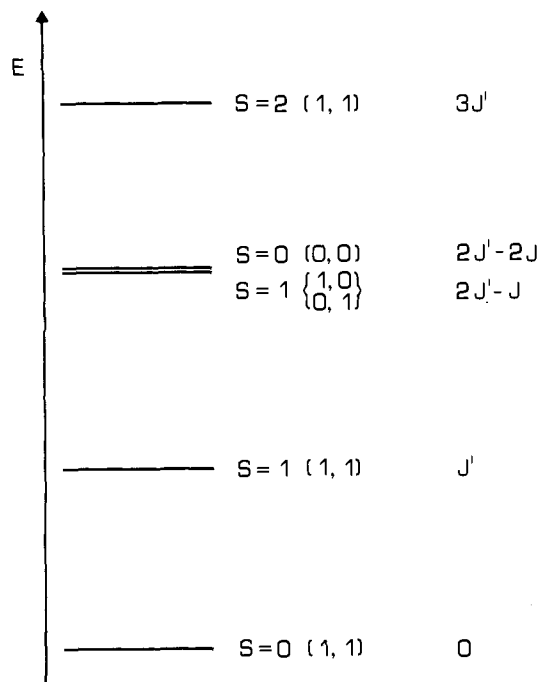
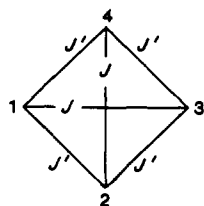


Figure 7. Order of the energy levels for I obtained from the analysis of the temperature dependence of the magnetic susceptibility.

large isotropic interaction ($J, J' \gg D_{ij}$), the total spin $S = S_1 + S_2 + S_3 + S_4$ is a good quantum number and so are the intermediate $S^* = S_1 + S_3$ and $S^+ = S_2 + S_4$. The energies of the states, which are labeled using S , S^* , and S^+ , are:

$$E(2,1,1) = \frac{1}{2}J + J' \quad (2)$$

$$E(1,1,1) = \frac{1}{2}J - J' \quad (3)$$

$$E(0,1,1) = \frac{1}{2}J - 2J' \quad (4)$$

$$E(1,1,0) = E(1,0,1) = -\frac{1}{2}J \quad (5)$$

$$E(0,0,0) = -\frac{3}{2}J \quad (6)$$

Therefore two spin singlets, three triplets, and one quintet are thermally populated. The relative energies as obtained from the analysis of the temperature dependence of the magnetic susceptibility are shown in Figure 7. Two of the triplets are degenerate. For each of the multiplets the g tensors are expressed according to the relation:

$$\mathbf{g} = \frac{1}{4}(\mathbf{g}_1 + \mathbf{g}_2 + \mathbf{g}_3 + \mathbf{g}_4) \quad (7)$$

while the A tensors of each individual paramagnetic center are $1/4$ the value the center would possess in a noncoupled system. In (7) we have not considered possible second-order effects which might show up in degenerate multiplets.⁵¹

The situation is more complicated for the zero-field splitting tensors of the $S = 2$ and $S = 1$ total spin multiplets, which can be expressed as linear combinations of the individual D_{ij} tensors. With an extension of a previously suggested procedure¹¹ it is found that:

$$D(S=2, S^*=S^+=1) = \frac{1}{12}(D_{12} + D_{13} + D_{14} + D_{23} + D_{24} + D_{34}) \quad (8)$$

$$D(S=1, S^*=S^+=1) = \frac{1}{4}(D_{12} + D_{14} + D_{23} + D_{34} - D_{13} - D_{24}) \quad (9)$$

The two degenerate triplets do have zero-field splittings, yielding in the most general case three sets of two degenerate levels in zero field. Also their splitting pattern is complicated, but since, on the basis of the magnetic susceptibility data, they are expected

to be largely depopulated at the temperature at which triplet spectra are observed, they will not be further characterized here.

It is useful at this point to make a more extensive use of the symmetry condition to simplify the above general relations. Indeed the following equations must hold for the components of the g and D tensors:

$$\begin{aligned} g_{1xx} &= g_{2yy} = g_{3xx} = g_{4yy} \\ g_{1yy} &= g_{2xx} = g_{3yy} = g_{4xx} \\ g_{1zz} &= g_{2zz} = g_{3zz} = g_{4zz} \\ g_{1xy} &= -g_{2xy} = g_{3xy} = -g_{4xy} \\ g_{1xz} &= g_{2yz} = -g_{3xz} = -g_{4yz} \\ g_{1yz} &= -g_{2xz} = -g_{3yz} = g_{4xz} \end{aligned} \quad (10)$$

and

$$\begin{aligned} D_{13xx} &= D_{24yy}, D_{12xx} = D_{14yy} = D_{23yy} = D_{34xx} \\ D_{13yy} &= D_{24xx}, D_{12yy} = D_{14xx} = D_{23xx} = D_{34yy} \\ D_{13zz} &= D_{24zz}, D_{12zz} = D_{14zz} = D_{23zz} = D_{34zz} \\ D_{13xy} &= -D_{24xy}, D_{12xy} = -D_{14xy} = -D_{23xy} = D_{34xy} \\ D_{13xz} &= D_{24yz}, D_{12xz} = -D_{14yz} = D_{23yz} = -D_{34xz} \\ D_{13yz} &= -D_{24xz}, D_{12yz} = D_{14xz} = -D_{23xz} = -D_{34yz} \end{aligned} \quad (11)$$

In (10) and (11) the x , y , and z axes correspond to the tetragonal axes. Using them in (7)–(9) we find that g , $D(2,1,1)$, and $D(1,1,1)$ are axial with: $g_{\parallel} = g_{1zz}$, $g_{\perp} = 1/2(g_{1xx} + g_{1yy})$, $D(2,1,1) = 1/2 D_{12zz} + 1/4 D_{13zz}$, $D(1,1,1) = 3/2 D_{12zz} - 3/4 D_{13zz}$.

With these tools in hand we can now proceed to the analysis of the EPR spectra. The g tensors of both the $S = 2$ and $S = 1$ spectra are identical within experimental error, as expected. In order to relate them to the individual g tensors it is necessary to have a closer look at the coordination environment of each copper ion and at the orientation of the molecular axes. Each copper ion is in a five-coordinate environment of four nitrogen and one oxygen atoms.⁴¹ The axial bond Cu–N5 defines the molecular z axis, which in the laboratory frame has direction cosines 0.6281, 0.7319, and 0.2642. If we assume for the sake of simplicity that the individual copper g_{Cu} tensor is axial, the experimental g_{\parallel} and g_{\perp} values are given by:

$$\begin{aligned} g_{\parallel} &= 0.0698g_{\parallel,Cu} + 0.9302g_{\perp,Cu} \\ g_{\perp} &= 0.4651g_{\parallel,Cu} + 0.5349g_{\perp,Cu} \end{aligned}$$

From this we calculate $g_{\parallel,Cu} = 2.34$ and $g_{\perp,Cu} = 2.01$. These values are in only fair agreement with what can be expected for square-pyramidal copper complexes,⁵² in particular the $g_{\perp,Cu}$ value is too small. This discrepancy might be due to the assumption of axial symmetry for g_{Cu} , but since symmetry allows us to determine only two experimental g values we cannot relax it.

The second spin-Hamiltonian parameter we have available is the hyperfine splitting observed in the triplet spectrum. At first it can be surprising to note that the hyperfine pattern corresponds to the interaction of the unpaired electrons with two rather than with four copper nuclei. However, this is easily understood if we look at the structure of the cluster. Indeed the orientation of the static magnetic field in which the maximum hyperfine splitting is observed corresponds to a direction which is almost parallel to the z molecular axis of the 1 and 3 copper ions. Therefore, for these two ions the hyperfine splitting must be roughly $1/4 A_{\parallel,Cu}$, while for the other two it must be $1/4 A_{\perp,Cu}$. Therefore, one should expect one septet of septets; since, however, $A_{\perp,Cu}$ is generally small, only one septet is resolved. The actual value of A , 0.0045 cm^{-1} , corresponds to $A_{\parallel,Cu} \approx 0.0180 cm^{-1}$, which can be considered satisfactory for a square-pyramidal copper complex. No hyperfine is resolved parallel to c in agreement with the fact that the mo-

lecular z axes are almost orthogonal to it.

It should be noted here that in the above discussion we have assumed that the triplet spectra belong to the Cu_4 cluster. They might also be due to a dinuclear impurity, but the above satisfactory explanation, together with the A value, which would be too small for an isolated pair of copper ions, confirms our assumption. The first excited triplet is 12.2 cm^{-1} above the ground singlet, while the two degenerate triplets are at 25.0 cm^{-1} . Since the triplet spectra are observed only below 10 K, we presume that they are associated with the ($S = 1, S^* = S^+ = 1$) state because in this range of temperatures the two degenerate triplets should be largely depopulated.

We are now in the position to analyze the zero-field splitting tensors of both the quintet and triplet states. It would be important to have the signs of D available, but unfortunately this is not the case, so that we must only assume them. We have on the whole four different possibilities to assign the sign of D for the $S = 2$ and $S = 1$ states. Using the relations given above we find two sets of D_{12zz} and D_{13zz} values, the values in each set differing for the signs. They are $D_{12zz} = +0.0077 cm^{-1}$, $D_{13zz} = +0.1363 cm^{-1}$ and $D_{12zz} = +0.0681 cm^{-1}$, $D_{13zz} = +0.0153 cm^{-1}$, respectively. There is no a priori reason why one set should be preferred to the other, but we are inclined to prefer the second one, which gives a smaller $|D_{13zz}|$ value. In fact, the copper ions 1 and 3 are not bridged directly like, for instance, Cu1 and Cu2, and also the Cu1–Cu3 distance is longer than that for Cu1–Cu2. Indeed the value of $|D_{12zz}| = 0.0681 cm^{-1}$ compares well with those observed for dinuclear copper complexes bridged in a similar fashion by triazolato ligands,⁵³ where the principal values of the D_{12} tensor were found to be 0.0052, 0.0676, and 0.0728 cm^{-1} , respectively. The Cu–Cu distance in that case was only slightly shorter,⁵⁴ 408.5 vs. 426.9 pm observed in the present case.⁴⁷

A useful check for these values can come also from the computation of the dipolar component of the D_{ij} tensors. In order to perform this within the point dipolar approximation, a precise knowledge of the individual g tensors should be available. Since, for the reasons outlined above, this is not the case, we performed sample calculations using isotropic g values and a procedure which has been justified in the analysis of the dipolar broadening mechanism in one-dimensional antiferromagnets.⁵⁵ Within this model we calculate $D_{12zz} = -0.0108 cm^{-1}$ and $D_{13zz} = 0.0243 cm^{-1}$. From this we see that the latter is reasonably close to the value obtained from the analysis of the EPR spectra, while the former is completely at large, showing that exchange-determined components are of paramount importance in determining the D_{ij} tensors, as previously observed for similar bridges.⁵³

We have assigned the transitions belonging to the $S = 2$ and $S = 1$ states originating from the interaction of $S^* = 1$ and $S^+ = 1$. The other paramagnetic state which is left is that of the two degenerate $S = 1$ multiplets, and we have two features observed in the low-temperature spectra, one at ca. 100 and the other at ca. 300 mT. The magnetic data suggest that at low temperature they should be practically depopulated, the calculated intensity ratio for the lowest triplet and the degenerate triplets at 4.2 K being 0.012. A possibility could be that of assigning the feature at $g = 2.06$ which we observe in the spectra to a $\Delta M = \pm 1$ transition of these degenerate triplets. However, against this assignment is the fact that the resonance field is independent of the orientation, while the expected g values should be identical with those of the other multiplets and anisotropic. Also the shape of the transition is anomalous, so it can be suspected that it can be due to some decomposition products of the crystal in the thermal treatment required to cool down the sample.

A safe explanation can neither be given for the line at ca. 100 mT. Its position at $g = 6$ might suggest a $\Delta M = \pm 3$ transition, but this could occur only for the $S = 2$ multiplet, and at low temperature it is depopulated.

(53) Bencini, A.; Gatteschi, D.; Zanchini, C.; Haasnoot, J. G.; Prins, R.; Reedijk, J. *Inorg. Chem.* **1985**, *24*, 2812.

(54) Prins, R.; Birker, P. J. M. W. L.; Haasnoot, J. G.; Verschoor, G. C.; Reedijk, J. *Inorg. Chem.* **1985**, *24*, 4128.

(55) McGregor, K. T.; Soos, Z. G. *J. Chem. Phys.* **1976**, *64*, 2508.

As an alternative one could suspect the presence of some impurity in which, for instance, a copper(II) ion is missing in the cluster, or to interactions between neighboring clusters in the triplet state, yielding $S = 1$ states. The second alternative might be confirmed by the presence of satellites flanking the $\Delta M = \pm 1$ transition at low temperature. Indeed similar absorptions were assigned to transitions between states generated by the interaction between neighboring molecules in the triplet state in the spectra of a copper(II) maleonitrile dithiolate analyzed by Keijzers et al.⁵⁶ The possibility of such interactions is supported by the extensive network of hydrogen bonds connecting different clusters. Since they appear clearly only in few crystal orientations we did not attempt further to characterize them.

In conclusion in the present work we have observed the EPR spectra of both a quintet and a triplet originated by the exchange interaction of four equivalent copper ions arranged on the vertices of a distorted tetrahedron of S_4 symmetry. We do not see any evidence of the spectra of the other two (degenerate) triplet states. The reason for this lies presumably in unfavorable relaxation time. In fact, the spectra of the lowest triplet shows up only below 10

K, broadening beyond detection at higher temperature. If the degenerate triplets have the same behavior, then their spectra are not observed because at high temperature, when they are populated, the relaxation is too fast, while at low temperature they are practically depopulated. The data in any case show that the relaxation in the triplets is much more effective than in the quintet state, which yields a measurable spectrum also at room temperature. Since the triplet spectra of isolated pairs of copper ions are generally well resolved also at high temperature, we suspect that the fast relaxation observed in this case is related to the presence of three states with the same spin multiplicity separated by ca. 20 cm^{-1} . It is worth noting that anomalous line-width behavior has been observed also for trinuclear copper complexes⁵⁷⁻⁵⁹ in which two doublet states are formed by the exchange interaction.

Acknowledgment. The authors are indebted to Professor Olivier Kahn (visiting Van Arkel Professor at Leiden, 1986) for helpful discussions, and to Mr. Cees Vada for many crystal growth efforts.

(56) (a) Snaathorst, D.; Doesburg, H. M.; Parenboom, J. A. A. J.; Keijzers, C. P. *Inorg. Chem.* **1981**, *20*, 2526. (b) Snaathorst, D.; Keijzers, C. P. *Mol. Phys.* **1984**, *51*, 509.

(57) Banci, L.; Bencini, A.; Gatteschi, D. *Inorg. Chem.* **1983**, *22*, 2681.

(58) Banci, L.; Bencini, A.; Dei, A.; Gatteschi, D. *Inorg. Chem.* **1983**, *22*, 4018.

(59) Benelli, C.; Bunting, R. K.; Gatteschi, D.; Zanchini, C. *Inorg. Chem.* **1984**, *23*, 3074.

The Geometry Factor in Photoprocesses on Irregular (Fractal) Surfaces. 1. Static Considerations

David Avnir

Contribution from the Department of Organic Chemistry and the F. Haber Research Center for Molecular Dynamics, The Hebrew University of Jerusalem, Jerusalem 91904, Israel.

Received September 17, 1986

Abstract: Surface geometry effects on photoprocesses of adsorbates are discussed, with special emphasis on problems which originate from surface irregularities of silica. It is shown that the common practice of idealizing irregular surfaces as flat ones leads to inaccuracies in the evaluations of a variety of adsorption parameters, such as effective surface area, the area occupied by one molecule, intermolecular distances, etc. Data from a number of recent reports in surface photochemistry is reanalyzed to demonstrate the possible errors and to show that the interpretation of results may be altered if the calculations are carried out without the flat surface assumption. These literature examples are the photodimerization of cyanophenanthrene, the chemiluminescent oxidation of fatty acids, the benzophenone triplet quenching, and the excimerization process in pyrenyl-derivatized silica. Calculation procedures for the above mentioned parameters on irregular surfaces are suggested based both on classical surface-science considerations and on recent fractal considerations. Computational simulations demonstrate the effect of surface irregularities on these parameters. The replacement of the flat picture with the real irregular one reveals a number of new interesting concepts: the effective surface area for reaction (the reaction area) is smaller than the effective surface area available to the reactants; the effective surface area toward an excited state adsorbed molecule is different than the ground-state case; the distance between a large and small molecule depends on which molecule diffuses toward the other; in bimolecular reactions, not all of the smaller molecules are available at any time to the larger ones. Surface heterogeneity and environmental relaxation around an excited state are discussed in terms of geometry.

1. Introduction

Photochemistry has reached a mature stage in which studies in homogeneous solutions gradually yield to studies under the more realistic conditions of heterogeneous environments. These heterogeneous environments can be fluid and flexible (water surfaces, micelles) or solid (surfaces). In this report I concentrate on the latter.

In trying to extrapolate the knowledge which has been accumulated in homogeneous photochemistry to the heterogeneous systems, one has to take into account two parameters: the physico-chemical properties of the environment and the geometrical details of the environment. These geometrical details should be taken into account both on small molecular scales of, e.g., cage

size and on larger diffusional scales (geometrical details on these two scales need not coincide). Extrapolation of the first parameter from homogeneous to heterogeneous environment has been straightforward: for instance, much of what is known about the hydrogen bond in solution can be applied directly to solid materials which have surface moieties capable of forming this bond.¹ It is the second parameter, the geometry, which is new and which cannot be extrapolated from solution studies. Whereas in solution, the environment is spherical-symmetric, reversible, and flexible, various geometries are possible around an adsorbed molecule, and

(1) Schuster, P.; Zundel, G.; Sandorfy, C. *The Hydrogen Bond*; North Holland: Amsterdam, 1976; Vol. 3.